Quaternary Science Reviews 310 (2023) 108123

Contents lists available at ScienceDirect

Quaternary Science Reviews

journal homepage: www.elsevier.com/locate/quascirev

Last glacial maximum cooling of 9 °C in continental Europe from a 40 kyr-long noble gas paleothermometry record

D.V. Bekaert [a, b, *], P.-H. Blard [a, c], Y. Raoult [a, d], R. Pik [a], R. Kipfer [e, f, g], A.M. Seltzer [b], E. Legrain [h], B. Marty [a]

[a] Université de Lorraine, CNRS, CRPG, F-54000, Nancy, France
[b] Marine Chemistry and Geochemistry Department, Woods Hole Oceanographic Institution, Woods Hole, MA, USA
[c] Laboratoire de Glaciologie, DGES-IGEOS, Université Libre de Bruxelles, 1050, Brussels, Belgium
[d] UMR 7619 METIS, Sorbonne Université, 4 Place Jussieu, 75005, Paris, France
[e] Institute of Biogeochemistry and Pollutant Dynamics, Department of Environmental Systems Science, Swiss Federal Institute Technology, ETHZ, Zurich, Switzerland
[f] Institute of Geochemistry and Petrology, Department of Earth Sciences, Swiss Federal Institute Technology, ETHZ, Zurich, Switzerland
[g] Department of Water Resources and Drinking Water, Swiss Federal Institute of Environmental Science and Technology (EAWAG), Dübendorf, CH-8600, Switzerland
[h] Université Grenoble Alpes, CNRS, IRD, IGE, Grenoble, France

ARTICLE INFO

Article history:
Received 13 December 2022
Received in revised form
31 January 2023
Accepted 5 May 2023
Available online 11 May 2023

Handling Editor: Giovanni Zanchetta

Keywords:
Noble gas paleothermometry
Continental Europe
Last glacial maximum
Climate sensitivity

ABSTRACT

The Last Glacial Maximum (LGM; ~26–18 kyr ago) is a time interval of great climatic interest characterized by substantial global cooling driven by radiative forcings and feedbacks associated with orbital changes, lower atmospheric CO2, and large ice sheets. However, reliable proxies of continental paleotemperatures are scarce and often qualitative, which has limited our understanding of the spatial structure of past climate changes. Here, we present a quantitative noble gas temperature (NGT) record of the last ~40 kyr from the Albian aquifer in Eastern Paris Basin (France, ~48°N). Our NGT data indicate that the mean annual surface temperature was ~5 °C during the Marine Isotope Stage 3 (MIS3; ~40–30 kyr ago), before cooling to ~2 °C during the LGM, and warming to ~11 °C in the Holocene, which closely matches modern ground surface temperatures in Eastern France. Combined with water stable isotope analyses, NGT data indicate δD/NGT and δ^{18}O/NGT transfer functions of +1.6 ± 0.4‰/°C and +0.18 ± 0.04‰/°C, respectively. Our noble-gas derived LGM cooling of ~9 °C (relative to the Holocene) is consistent with previous studies of noble gas paleothermometry in European groundwaters but larger than the low-to-mid latitude estimate of 5.8 ± 0.6 °C derived from a compilation of noble gas records, which supports the notion that continental LGM cooling was more extreme at higher latitudes. While an LGM cooling of ~9 °C in Eastern France appears compatible with recent data assimilation studies, this value is greater than most estimates from current-generation climate model simulations of the LGM. Comparing our estimate for the temperature in Eastern France during MIS3 (6.4 ± 0.5 °C) with GCM outputs presents a promising avenue to further evaluate climate model simulations and constrain European climate evolution over the last glacial cycle.

1. Introduction

Constraining the evolution of past climate is key for evaluating modern estimates of equilibrium climate sensitivity (ECS) and improving predictions of future climate change. For decades, our understanding of past climate evolution has improved thanks to the analysis of polar ice cores (e.g., Lorius et al. (1990); Dansgaard et al. (1993); Petit et al. (1999)) and oceanic sediment archives (e.g., McManus et al. (1999); Peterson et al. (2000); Martrat et al. (2007)). Both archives have the advantage of providing near continuous high-resolution records of paleoclimatic information. The analysis of air bubbles trapped in ice cores notably helped unraveling the role of CO_2 in driving and/or amplifying global

* Corresponding author. Université de Lorraine, CNRS, CRPG, F-54000, Nancy, France.
E-mail address: david.bekaert@univ-lorraine.fr (D.V. Bekaert).

https://doi.org/10.1016/j.quascirev.2023.108123
0277-3791/

climate variations (Caillon et al. (2003); Shakun et al. (2012); Parrenin et al. (2013)). However, polar and marine paleoclimate records alone are insufficient to determine the spatial structure of climate changes at Earth's surface, especially on the continents. The development of quantitative proxies of continental paleoclimates is essential to constrain the magnitude and spatial structure of past climate changes in terrestrial regions that are heavily populated today (e.g., Cleator et al. (2020); Seltzer et al. (2021a)).

One of the best-documented, geologically-recent global climate transitions is the last deglaciation, that started ~20 kyr ago, when the Earth transitioned from a ~100 kyr-long glacial period. The last glacial maximum (LGM; ~26 kyr ago if defined by the strict maximum in global ice volume (Grant et al. (2014)) was characterized by low levels of pCO_2 (~185 ppm), which subsequently increased to pre-industrial levels (~280 ppm) in conjunction with rising global temperatures (e.g., Parrenin et al. (2013)). For this reason, paleoclimatologists have long sought to refine estimates of regional temperature changes during the LGM as a way to constrain Earth's ECS. It is however worth noting that the very definition of the LGM may vary slightly across scientific communities. Defining the LGM in a way that integrates constraints from geomorphological records of glaciations, changes in global sea level, and $\delta^{18}O$ signals in the marine record has proven challenging (Clark et al. (2009); Hughes and Gibbard (2015)). Overall, estimates for the timing of the LGM across the globe spread over more than 10 kyr (Shakun and Carlson (2010)), implying that a distinction must often be made between local, regional, and global "LGMs". Here we consider the global LGM period to range from 28 to 23 kyr ago, as defined by (Hughes and Gibbard (2015)) as the maximum of global ice volume and atmospheric dust concentration.

Recent data assimilation studies of the LGM have incorporated large collections of sea surface temperature (SST) proxy to simulate the spatial distribution of surface temperature changes since the global LGM (Tierney et al. (2020); Osman et al. (2021)). As a way to assess the validity of the simulation outputs, these results are compared with independent ice core and speleothem $\delta^{18}O$ data (Tierney et al. (2020)). Although many terrestrial paleoclimate archives exist (e.g., fossil pollen records (Bartlein et al. (2011); Cleator et al. (2020)), speleothems (James et al. (2015)), glacier equilibrium lines (e.g, Porter (2000); Martin et al. (2020)), noble gases in groundwater (Stute et al. (1995)), these have been largely overlooked in most data assimilation studies, leading to large uncertainties about the magnitude and dynamics of past climate changes in populated regions. The main reason for ignoring these paleoclimate proxy data is that most of them do not provide quantitative, reliable, and spatially-distributed estimates of past temperatures.

In multiple regions of the globe, existing LGM paleotemperature records from terrestrial proxies exhibit disagreements potentially attributed to proxy specific biases. At low elevation, historical pollen data have for instance been used to suggest a tropical cooling $\leq$3 °C during the LGM (e.g., Bartlein et al. (2011)), whereas noble gas abundances in groundwater indicate a larger LGM tropical cooling of 5.8 ± 0.6 °C (Stute et al. (1995); Seltzer et al. (2021a)). At higher elevations (>3000 m), LGM glacier equilibrium lines (Porter (2000); Blard et al. (2007)) and organic matter in lakes (Loomis et al. (2017)) also suggest large tropical cooling, from ~6 to 9 °C. These apparent discrepencies could potentially reflect an amplification of LGM cooling (and thus, of equilibrium warming) with altitude (lapse rate) or distance from the shoreline (continental amplification). Loomis et al. (2017) for instance proposed that their estimate of LGM tropical cooling from organic matter in lakes could be compatible with a ~2 °C LGM cooling at low elevation (i.e., sea level), consistent with pollen paleoclimatic records (Bartlein et al. (2011)). Such a low estimate of LGM tropical cooling at low elevation is however inconsistent with most noble gas reconstructions (Seltzer et al. (2021a)). Recently, Cleator et al. (2020) presented a new global reconstruction of LGM seasonal climates using data assimilation of pollen records with the ensemble average of the PMIP3—CMIP5 simulations. This new reconstruction yielded a larger tropical LGM cooling (~4.7 °C) than previous pollen-based reconstructions (Bartlein et al. (2011)), in closer agreement with independent constraints from noble gas records (Seltzer et al. (2021a)). The same potential complications of proxy specific biases and vertical or continental amplifications of equilibrium warming arise for the mid-to high-latitude regions, where estimates of LGM cooling are even more variable than in the tropics (Seltzer et al. (2021a)). While the polar amplification of climate change is a robust feature of model simulations (e.g., Holland and Bitz (2003); Pithan and Mauritsen (2014)) and data (Tierney et al. (2020)), the cause(s) and latitudinal extent of polar amplification remain debated (Stuecker et al. (2018)). These considerations underline a crucial need for robust paleotemperature reconstructions of glacial cooling at mid-to high latitudes, in the continental realm.

Due to their temperature-dependent solubilities in water and insensitivity to biological and chemical processes, noble gases dissolved in ancient groundwater have long been recognized as a reliable archive of past climates, with a well established, quantiative link to past land surface temperatures (e.g. Aeschbach-Hertig et al. (2000); Mazor (1972); Stute et al. (1995); Loosli et al. (2001); Aeschbach-Hertig and Solomon (2013)). Today, about a third (27.0—36.3%) of Earth's land area is estimated to hold LGM-aged groundwater (Befus et al. (2017)). By applying a physical recharge model that account for both the temperature-dependent solubility equilibrium between air and water, as well as bubble injection and partial dissolution (Ingram et al. (2007)), measured noble gas concentrations can be interpreted with an inverse model to quantitatively reconstruct past Mean Annual Surface Temperatures on land (MAST, (Aeschbach-Hertig and Solomon (2013)). Here, we present a brief summary of the noble gas thermometry approach, and report a new ~40-kyr long noble gas record of past MAST from the Albian aquifer of the Paris Basin, in Eastern Fance. We use these new data to discuss the spatial gradients of equilibrium warming across Western Europe (as a function of altitude, latitude, and distance from the shore), and to assess the capability of atmospheric global climate model (GCMs) to reproduce past LGM conditions.

2. Material and methods

2.1. Noble gas thermometry

The early recognition that the stable isotope composition of water molecules in rainwater (i.e., $\delta^{18}O$ and δD) depends on several climatic factors, including air temperature, rain amount, altitude, and latitude of precipitations (e.g., Craig (1961)) paved the way for isotope hydrology and hydroclimatology. Dissolved atmospheric neon (Ne), argon (Ar), krypton (Kr) and xenon (Xe) concentrations in groundwater have long been recognized as reliable proxies of past climate, with a physics-based link to past land surface temperature (e.g. Mazor (1972); Stute et al. (1995); Loosli et al. (2001); Seltzer et al. (2021a)). Because atmospheric noble gases are inert and lack appreciable sinks or sources, their concentrations in fresh water at solubility equilibrium reflect well-understood physical constants that primarily depend on temperature, barometric pressure, and "additional" dissolved noble gases acquired by bubble entrainment and dissolution during recharge (referred to as "excess air" or "ΔNe", because neon is a sensitive indicator of excess air dissolution owing to its low solubility (Andrews and Lee (1979); Heaton and Vogel (1981); Klump et al. (2008)). Owing to the

attenuation of seasonal temperature fluctuations in soil with depth, typical temperatures at the water table (that is, the upper surface of the saturated zone) closely match MAST (Aeschbach-Hertig and Solomon (2013)). In most cases, MAST appear to be 1–2 °C warmer than Mean Annual surface Air Temperatures (MAAT) (Seltzer et al. (2021a)), with slight decoupling notably arising at high latitudes due to changes in snow cover or vegetation (e.g., Stute and Sonntag (1992)). However, changes in MAST and MAAT can be reasonably assumed to be of equal magnitudes, such that ΔNGT_{LGM} are directly comparable to MAAT changes since the LGM.

When groundwater is isolated from soil air by subsequent recharge or flow beneath a confining layer, dissolved noble gases are preserved. Because they lack subsurface sources or sinks, the concentrations (of Ne, Ar, Kr, and Xe) are preserved after the time of recharge and affected only by dispersive mixing and advection. Unlike stable noble gases, atmosphere-derived radioactive isotopes in groundwater will decay according to their respective half-lives (e.g. $t_{1/2}$ (^{14}C) = 5730 yr), providing a way to determine both **(i)** the "age" of groundwater recharge from the activities of radioactive species, and **(ii)** the noble gas temperatures (NGT) from bulk noble gas concentrations. Although the 5730 year half-life of ^{14}C and the ubiquity of carbon in groundwater make it a powerful - and widely applied - age tracer on the timescale of ~1000 to ~40 000 years, the potential for hydrogeochemical reactions and physical processes to alter measured ^{14}C activities (Geyh (2000)) require caution when interpreting ^{14}C-dated sample chronologies.

Over the past ~40 yr, multiple noble gas studies have aimed at **(i)** improving numerical approaches to deconvolve "excess air" and "equilibrium" (i.e., temperature) signals in groundwater data, and **(ii)** reconstructing glacial/interglacial NGT changes across the continents (e.g., Edmunds and Milne (2001); Corcho Alvarado et al. (2011); Seltzer et al. (2021a) and *references therein*). Multiple conceptual models (e.g., unfractionated air (UA) (Heaton and Vogel (1981)), partial re-equilibration (PR) (Stute et al. (1995)), and oxygen depletion (OD) (Hall et al. (2005))) have been proposed to account for the variable compositions of soil air and excess air at the water table, including the variable extents of air entrapment and bubble dissolution during recharge (Klump et al. (2008)). Today, however, it is the so-called closed-system equilibration (CE) model (Aeschbach-Hertig et al. (2000)), whereby water table fluctuations entrain bubbles of soil air that partially dissolve under elevated hydrostatic pressure at solubility equilibrium, that has been established as the most robust and reliable approach (Kipfer et al. (2002); Aeschbach-Hertig and Solomon (2013)). Using late Holocene groundwater noble gas data from 30 study areas worldwide, Seltzer et al. (2021a) showed that CE model NGTs closely match modern ground surface and shallow groundwater temperature measurements, further demonstrating the robustness of this approach to using groundwater noble gases as an unbiased palaeothermometer.

2.2. Groundwater sampling of the Albian aquifer

The Albian aquifer of the Paris Basin (France), which has been exploited since 1841, shows drastic drawdown with a clear cone of piezometric depression near the Paris region, where ~23 × 10^6 m^3 of water are extracted every year for human use (cumulative volume abstraction of >450 × 10^6 m^3 over the period 1841–1935; Contoux et al. (2013)), among which ~80% are for domestic/human use. Water parcels from several flowlines converge towards this zone, where they mix with the underlying aquifer of Neocomian age (Fig. 1). More generally, the Albian aquifer consists of alternating layers of sand and clays, with a total porosity between 3% and 35% (average 25%) and a kinematic porosity – i.e., the porosity that actually contributes to the flow network – around 15%. The rate at which groundwater can flow through the Albian aquifer (referred to as transmissivity) has been previously estimated to be in the range [3.2–7.2]x10^{-5} m^2/s (Raoult (1999)).

Water samples from the Albian aquifer have been collected in the late 1990s, in the frame of the Raoult et al. (1998) project. We present here the results from water samples collected in 17 wells distributed along a South–North/West transect of the Paris Basin (average recharge elevation of 270 m), parallel to the subhorizontal flowlines of the aquifer (Fig. 1). Two samples (Ns1 and Ns2) originate from the Neocomian aquifer, and two others (Cs1 and Cs2) originate from a shallower aquifer associeted with chalk Raoult (1999)). All of the other samples originate from the Albian aquifer. Water samples dedicated to radiocarbon (^{14}C) dating were prepared by precipitating carbonates ($CaCO_3$ and $BaCO_3$, via $BaCl_2$ addition) from 80 L water containers, previously set at pH = 12 by NaOH addition. Radiocarbon activity was then measured using a conventional liquid scintillation analyzer; all ^{14}C ages were here calibrated using the most recent IntCal20 calibration curve (Reimer et al. (2020)). $\delta^{13}C$ was measured from CO_2 released under vacuum from 100-mL water samples via addition of H_3PO_4. Radiocarbon and $\delta^{13}C$ were measured at the Center de Recherches Géodynamiques (Thonon-les-Bains, France) following the procedure described by Olive (1999). $\delta^{18}O$ and δD values were determined at the Laboratoire de Biochimie isotopique (Université Paris VI) following procedures described by Gat and Gonfiantini (1981) and Coleman et al. (1982), respectively. Water samples collected in 3/8" copper tubes were analyzed at ETH Zurich for noble gas abundance determination (i.e., ^3He, ^4He, ^{20}Ne, ^{36}Ar, ^{40}Ar, ^{84}Kr, ^{132}Xe), following the procedure described by Weyhenmeyer et al. (2000). The conversion of noble gas abundances in groundwater into past temperatures was carried out assuming the closed-system equilibration (CE) model using the software PANGA (Jung and Aeschbach (2018)), and compared to results from a recent approach by Seltzer et al. (2021a).

3. Results

All data (^{14}C, δD, $\delta^{18}O$, noble gases, computed recharge paleotemperature) are reported in Tables S1–S5. The spatial distribution of ^{14}C activity within the Albian aquifer indicates that water parcels range in age from ~40 kyr ago (near the detection limit of radiocarbon) down to present-day (~90 pmc) with a general decrease of ^{14}C activity towards the center of the Paris Basin (Raoult et al. (1998)), consistent with previous ^{14}C measurements of the Albian aquifer (Vuillaume (1971)) and hydrological models of the Paris Basin (Castro et al. (1998)). The absence of notable $\delta^{13}C$ variations across all of our samples as well as their negative values well below 0‰ VPDB (with most data falling within the range of −15‰ to −10‰ VPDB) indicates that no significant correction for dead carbon input via carbonate dissolution is required in the present case (Fig. 2a). In detail, the highest DIC concentrations and highest $\delta^{13}C$ values appear in samples with the highest ^{14}C activites (Table S4). Among older samples, the lack of apparent trend in either DIC nor $\delta^{13}C$ with ^{14}C activity (Fig. S5) indicates that (a) input of ^{14}C-free DIC is not a major concern for dating, and (b) the younger groundwaters likely have a distinct source of DIC than groundwater samples from the Albian aquifer (perhaps from agricultural infuence via seepage of irrigation water to shallow groundwater; e.g., Seltzer et al. (2021b)). However, if the addition of ^{14}C-free DIC was biasing ^{14}C ages towards low values in the Albian aquifer, then the highest DIC should be associated with the oldest samples, which is not observed (Fig. S5). Thus, there is no basis for making a correction for dead carbon addition in the present case.

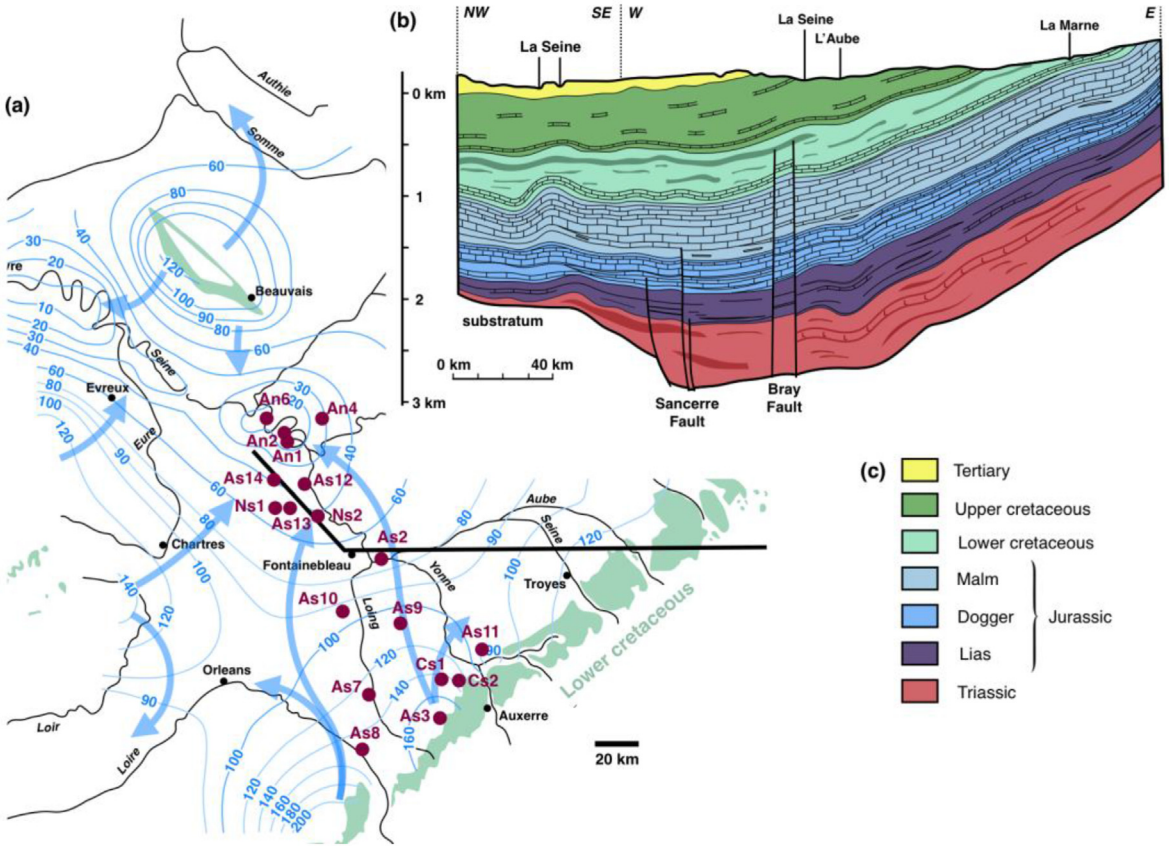

Fig. 1. Location of groundwater sampling sites in the Paris Basin. (a) Piezometric map of the Paris Basin showing the flowlines in the confined Albian aquifer (cretaceous inf.) and piezometric contour (given in meters below surface). Sample names correspond to: A = Albian, N= Neocombian, C = "chalk", s = South, n = North. **(b)** Cross section of the Paris Basin (broadly following the cross section profile reported on panel (a)). **(c)** Stratigraphic levels represented on the cross section of panel (b). The Albian aquifer is located on the upper part of the Lower cretaceous. Adapted from Raoult (1999).

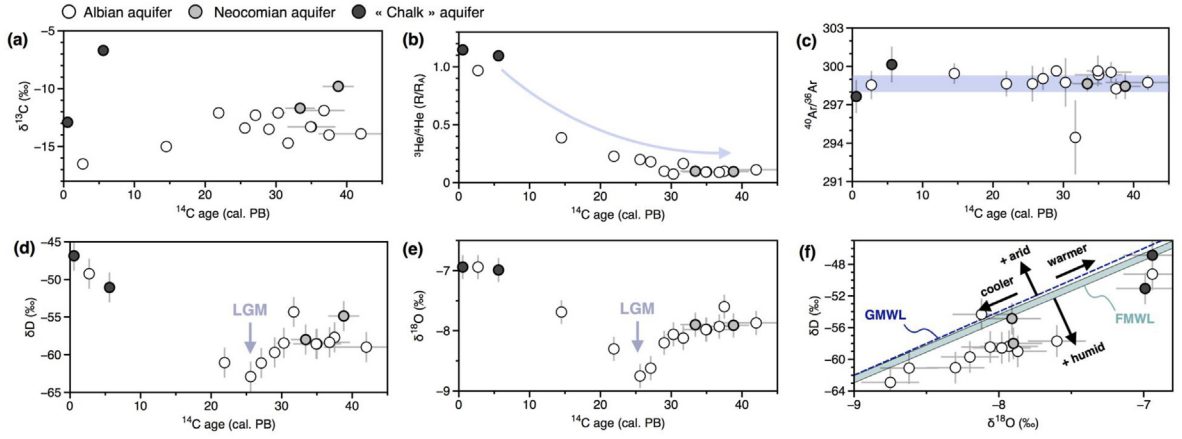

Fig. 2. Evolution of geochemical parameters in the Albian aquifer, as a function of ^{14}C age. Evolution of δ^{13}C (‰ VPDB) (a), He isotope ratios (b) (here given as R/R_A, where R and R_A correspond to the ^{3}He/^{4}He of the sample and atmosphere, respectively; Boucher et al. (2018)), ^{40}Ar/^{36}Ar (c), δD (‰ SMOW) (d) and δ^{18}O (‰ SMOW (e), as a function of calibrated ^{14}C age. **(f)** Groundwater stable isotope composition relative to the Global Meteoritic Water Line (GMWL) and French Meteoritic Water Line (FMWL) (Millot et al. (2010)).

The absence of evidence for dead carbon input via carbonate dissolution in the Albian aquifer is notably consistent with the paucity of carbonated lithologies within this aquifer.

The decreasing He isotope ratios of groundwater as a function of ^{14}C age (from R/R_A ~1 down to $\leq$ 0.1, where R and R_A correspond to the ^{3}He/^{4}He of the sample and atmosphere, respectively; Boucher et al. (2018)) reflects the progressive addition of radiogenic ^{4}He from U–Th decay along the water flowline (Fig. 2b). Conversly, the absence of significant ^{40}Ar/^{36}Ar evolution as a function of ^{14}C age indicates that, if present, the potential effect of ^{40}Ar* additions from ^{40}K decay is here below detection (Fig. 2c). The evolutions of δD (Fig. 2d) and δ^{18}O (Fig. 2e) as a function of ^{14}C age indicates that groundwater parcels analyzed in this study hold a paleoclimatic signal, with lighter δ^{18}O and δD in the glacial period relative to the Holocene, and the lowest values corresponding to the LGM. The stable isotope compositions of Albian groundwater plot very close

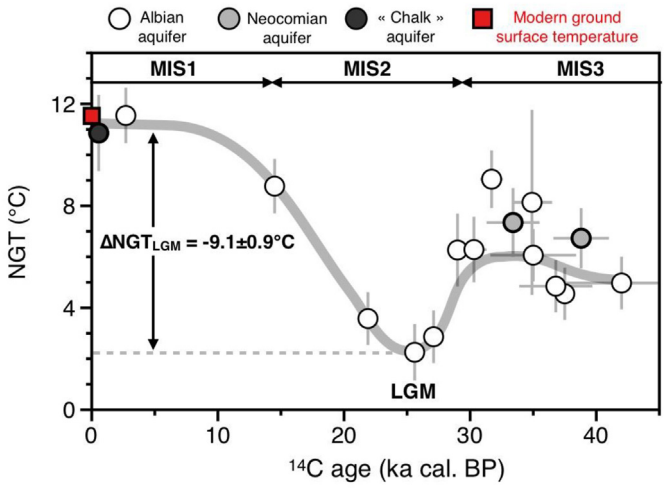

Fig. 3. Noble gas paleotemperature (NGT) computed using the closed-system equilibration (CE) model, a function of ^{14}C age (in kyr ago cal. BP). The NGT record depicts a clear temporal trend, from ~5 °C between 42 and 30 kyr ago down to ~2 °C between 28 and 25 kyr ago, and then up to a steady ~11 °C for the last 10 kyr (in excellent agreement with the average modern (1950–2019) ground surface temperature (red square) of 11.53 °C in Eastern France, as derived from ERA5-Land reanalysis (Hersbach et al. (2020)). The ΔNGT_{LGM} of −9.1 ± 0.9 °C is computed following approach by Seltzer et al. (2021a). Recharge elevation for PANGA calculations is taken at 271 m (i.e., P = 0.9680 atm). NGT reconstructions using the UA model are given for comparison in Fig. S1.

to the Global Meteoritic Water Line (GMWL) and French Meteoritic Water Line (FMWL) (Millot et al. (2010)), indicating limited – if any – evaporative loss, in line with a meteoritic origin of groundwater in the Albian aquifer (Innocent et al. (2021)).

Noble gas paleotemperatures (NGT) computed with the CE model using the software PANGA (Jung and Aeschbach (2018)) show a clear temporal trend (Fig. 3) that mimics the evolutions of δD (Fig. 2d) and $\delta^{18}O$ (Fig. 2e), from consistent NGTs ~6 °C between 42 and 30 kyr ago (i.e., during the Marine Isotope Stage 3, MIS3) down to ~2 °C between 28 and 25 kyr ago (MIS2), and then up to a steady ~11 °C for the last ~10 kyr (Fig. 3). These Holocene temperatures are in excellent agreement with the average modern (1950–2019) ground surface temperature of 11.53 °C in Eastern France, as derived from ERA5-Land reanalysis (Hersbach et al. (2020)). However, we note that two samples analyzed in this study appear to have been affected by degassing, as reflected in the occurrence of F values $\gg 1$ (Table S6). In the CE model, the dimensionless parameter F (also referred to as the "fractionation parameter") corresponds to the ratio between B (the final trapped gas to water volume ratio) and A (the volume ratio of air entrapped in the groundwater in the recharge zone to water) (e.g., Aeschbach-Hertig and Solomon (2013)). Hence, the model describes excess air for $F < 1$ and degassing for $F > 1$. While several samples reported in this study yield F values < 1, potentially attributed to the occurrence of excess air, the conspicuous occurrence of degassing in several samples prevents interpretation of potential excess air signatures. However, the observation that, despite their variable F values (Table S1), samples of similar ages yield consistent NGTs (Fig. 3) indicates that NGT reconstructed in this study are not significantly affected by degassing or potential excess air corrections.

4. Discussion

4.1. Comparison with previous NGT reconstructions in Europe

Our data indicate that the LGM in Eastern France was characterized by a MAST cooling (ΔNGT_{LGM}) of about −9 °C, similar to the glacial cooling of −8.4 ± 1.1 °C recorded in Belgian groundwater (Blaser et al. (2010); Fig. 4d). To date, ΔNGT_{LGM} reconstructions in Europe have shown significant variability, with for instance lower ΔNGT_{LGM} in Portugal (−5.9 ± 1.6 °C, De Melo Condesso et al. (2001); Fig. 4c) and England (−5.9 ± 1.1 °C, Andrews and Lee (1979); Fig. 4d) compared to "continental" Europe (Seltzer et al. (2021a)). Although Portugal and England are further South and West than Eastern France, respectively, these discrepencies could reflect spatial gradients of LGM cooling, controlled at the first-order by a continental amplification of equilibrium warming at increasing distances from the shoreline (e.g., Sutton et al. (2007); Byrne and O'Gorman (2018)). However, gaps in recharge during cold periods of permafrost have been suggested for the England record (Andrews and Lee (1979)), implying that the true LGM cooling for this region may be greater than 6 °C. Two paleo-reconstructions of NGT from Hungary also yielded contrasted ΔNGT_{LGM} (−6.5 ± 0.9 °C and −9.2 ± 1.0 °C; values recently updated by Seltzer et al. (2021a) using the datasets

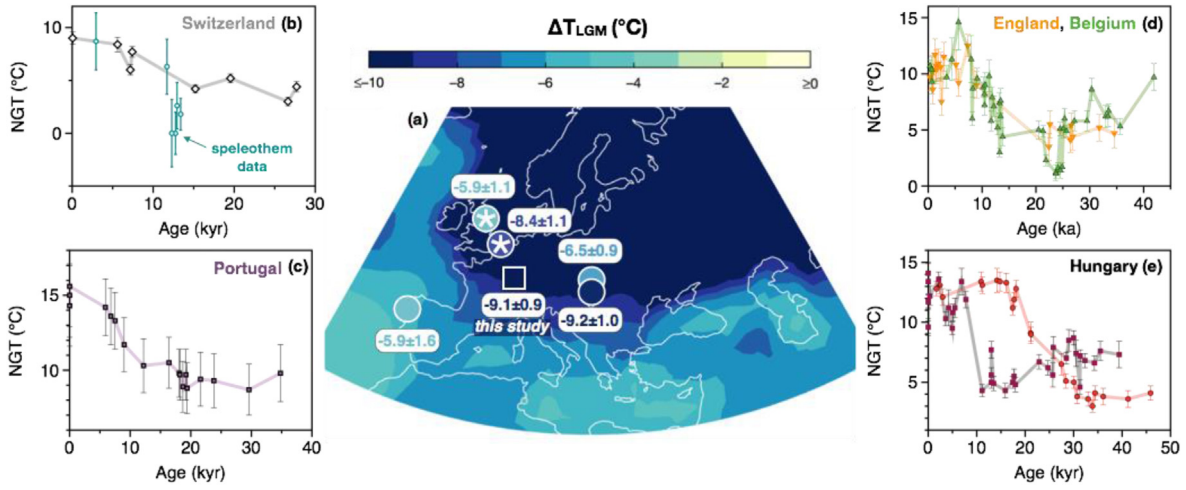

Fig. 4. NGT reconstructions across Europe and comparison of corresponding ΔNGT_{LGM} with results from the data assimilation results of Tierney et al. (2020) plotted using the MATLAB Mapping Toolbox following Seltzer et al. (2021a). Asterisks indicate sites with LGM recharge gaps, which coincide with the lateral extent of the LGM ice sheet (Stadelmaier et al. (2021)). NGT records from **(b)** Switzerland groundwater (Beyerle et al., 1998) and speleothem data (Ghadiri et al. (2018)) **(c)** Portugal (De Melo Condesso et al. (2001)), **(d)** England (Andrews and Lee (1979)) and Belgium (Blaser et al. (2010)), and **(e)** Hungary (Stute and Deak (1989); Varsányi et al. (2011)).

of Varsányi et al. (2011) and Stute and Deak (1989), respectively) as well as very different deglaciation timelines (Fig. 4e), emphasizing potential methodological bias, or more probably, issues with age models (Varsányi et al. (2011)). Overall, a LGM cooling of about −7 to −9 °C has been found previously by noble gas studies in Hungary, comparable to the magnitude of glacial cooling found in Belgium and Eastern France. Although more observations are required to draw a definitive conclusion, this dataset suggests a limited effect of continental amplification across central Europe.

Determining ΔNGT_{LGM} in Switzerland (intermediate location between Belgium-France and Hungary) has proven challenging given the difficulties in identifying LGM groundwaters in this mountainous area (Beyerle et al. (1998)) (Fig. 4b). Over the last decades, important analytical efforts have been achieved to extract and quantify noble gases from speleothem fluid inclusions, and derive NGTs (proxy of cave temperature) with a similar precision to groundwater data (after deconvolution of air-filled vs. water-filled inclusion signals) (e.g., Kluge et al. (2008); Vogel et al. (2013)). This promising approach enabled NGT's application to Holocene stalagmites in Switzerland for paleo-temperature reconstructions (e.g., Ghadiri et al. (2018), Fig. 4b) and investigations of past temperature–altitude gradients (Ghadiri et al. (2020)). Applying this technique to LGM-aged speleothems is a promising approach that could better constrain the amplitude of glacial cooling in the continental realm, at higher altitudes than groundwater noble gas data.

4.2. Comparison with other paleoclimate proxy data

A ΔNGT_{LGM} of about −9 °C in Eastern France is consistent with pollen-stratigraphic records from La Grande Pile and Les Echets (−10 ± 2 °C, Eastern France; Guiot et al. (1989)), as well as with the −7.8 to −11 °C cooling derived from inversion of the paleo-ice extent over the European Alps during the LGM (Višnjević et al. (2020)). Since our NGT record reflects temperatures of <500 m elevation, the agreement with glacier equilibrium line temperatures (reflecting paleoclimate at altitudes >1000 m) is a particularly interesting observation, as it would suggest a preservation of the vertical temperature gradient (i.e., the lapse rate) during the LGM, in Western Europe. However, this conclusion should be considered with caution given the relatively small altitudinal range covered by these two records. Systematic comparisons between low- and high-altitude paleotemperature reconstructions are required to determine whether the lapse rate was steeper during the LGM (i.e., amplification of glacial cooling with altitude (Blard et al. (2007); Loomis et al. (2017)), or indeed similar to present-day (Tripati et al. (2014); Banerjee et al. (2022)). Remarkably, a ΔNGT_{LGM} of −9 °C for Eastern France appears in line with recent data assimilation studies that developed field reconstructions of global LGM temperatures (Tierney et al. (2020)) from a large collection of geochemical paleo-SST proxies (Fig. 4). This finding potentially extends the low-to-mid latitude (<30°N) terrestrial proxy support for this recent SST-based simulation (Seltzer et al. (2021a)) to high latitude continental lands, like Eastern France. Including continental ΔT_{LGM} records (such as NGTs) in future efforts to synthesize global proxy data and simulate climate changes since the LGM (Tierney et al. (2020)) is a promising opportunity to assess and improve our understanding of terrestrial climate dynamics.

4.3. Temperature sensitivity of water stable isotopes and D-excess

The temporal evolution of NGT derived for the Albian aquifer using the CE model (Fig. 3) broadly mimics the evolutions of δD (Fig. 2d) and $\delta^{18}O$ (Fig. 2e), suggesting that these can be interpreted altogether in order to document past climates (Fig. 5). Variations in

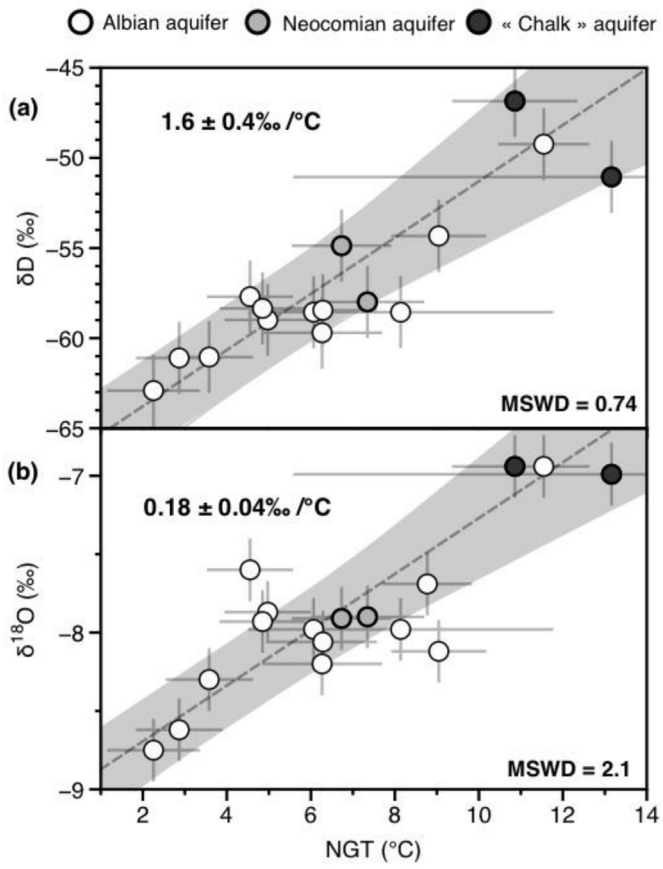

Fig. 5. δD and $\delta^{18}O$ as a function of NGT. Linear regressions (δD = (1.6 ± 0.4) x NGT - (66.9 ± 2.5) and $\delta^{18}O$ = (0.18 ± 0.04) x NGT - (9.1 ± 0.3)) were computed using the error weighted least squares algorithm of York et al. (2004).

the stable isotopes of water are however challenging to interpret by themselves as they may reflect multiple processes, including changes in temperature, moisture source(s), evaporation rates, precipitation amount, and atmospheric convection, which may all vary seasonally, annually and spatially (e.g., Dansgaard (2012); Rozanski et al. (1992); Araguás-Araguás et al. (2000)). Here, we observe that NGTs are linearly correlated with both δD (Fig. 5a) and $\delta^{18}O$ (Fig. 5b), indicating that temperature (rather than precipitation amount) is likely to be the main parameter controlling the evolution of water stable isotopes in Eastern France since the LGM. Although the exact series of mechanisms linking water stable isotope variations in precipitations to local temperature (as well as spatial temperature gradients) remain complex, the strong correlations between NGTs and water stable isotopes since MIS3 potentially open the door to using water stable isotope variations in precipitation as an empirical paleothermometer in other paleoclimate studies (e.g., using lake sediment archives (Leng and Marshall (2004))). Here, we compute linear δD/NGT and $\delta^{18}O$/NGT transfer functions of +1.6 ± 0.4‰/°C and +0.18 ± 0.04‰/°C, respectively. On the one hand, these values are markedly lower than those that have been previously considered to calculate paleotemperatures from the analysis of water stable isotope in speleothems fluid inclusions from Central Europe (2.88–4.80‰/°C for δD and 0.36–0.60‰/°C for $\delta^{18}O$; Affolter et al. (2019)). These $\delta^{18}O$/NGT transfer functions were derived by comparing $\delta^{18}O$ in modern precipitation and corresponding temperature time series for the *Global Network of Isotopes in Precipitation* stations in Basel (1986–2017) and Bern (1971–2017), and then considering

equilibrium fractionation factor of eight to transpose $\delta^{18}O$ in δD values (Affolter et al. (2019)). On the other hand, the $\delta^{18}O$/NGT derived in this study is markedly greater than the transfer function of 0.0708 ± 0.0034‰/°C computed from the paleoclimate data assimilation outputs of Osman et al. (2021) for the grid cell corresponding to our study area (Lat: 48.3, Lon: 5), over the last 23.9 kyr (Fig. S2). These discrepancies underline the fact that the exact temperature sensitivity of water stable isotopes in precipitations remains underconstrained, hence calling for extra caution when using $\delta^{18}O$ as a quantitative paleothermometer (Affolter et al. (2019)). Importantly, we note that changes in the seasonality between the last glacial period and the present day may have modified the transfer functions between water stable isotopes and temperature. For instance, an enhanced seasonality during the LGM in comparison to the late Holocene (Ford et al. (2015)) would cause winter precipitations to become a relatively smaller contributor to annual precipitations, thus affecting the slope of the $\delta^{18}O$/T relationship and biasing the weighted annual mean $\delta^{18}O$ of paleowaters towards the (higher) $\delta^{18}O$ of summer precipitations.

At last, since δD and $\delta^{18}O$ are highly correlated with temperature and with one another in our study (Figs. 2 and 5), the deuterium excess (D-excess $= \delta D - 8 \times \delta^{18}O$) appears rather invariant in time (Fig. S3), consistent with previous comparisons of water isotope systematics in modern infiltration waters and in old groundwaters in Western and Central Europe (e.g., Rozanski (1985)). Because D-excess is typically used as an indicator of both the source of precipitation and the conditions during vapor transport (e.g., Froehlich et al. (2002)), a constant D-excess excess over the last ~40 Myr is indicative of no major change in the moisture source of precipicipations over the study area since the last glacial period.

4.4. Comparison with global Climate model outputs

SST changes since the last glacial cycle are rather well documented (e.g., Ho and Laepple (2015)), with different temperature proxies yielding quite comparable LGM cooling from 2 °C (under the tropics) down to 5 °C at high latitudes. As discussed in this study, in-land proxies of paleotemperatures since the LGM suggest significant on land variability, and so the spatial evolution of equilibrium warming on the continental realm remains shrouded in uncertainty. Recently, a new generation of global climate models has been used to generate LGM simulations in the Paleoclimate Modelling Intercomparison Project (PMIP 4) contribution to the Coupled Model Intercomparison Project (CMIP) (Kageyama et al. (2021)). Most of these GCM experiments (as well as previous generation of simulations) yield significantly warmer LGM temperatures in Eastern France (48°N, 4°E) than our ΔNGT_{LGM} reconstuction (Fig. 6). Four models (HadCM3-PMIP3, CESM1-2, INM-CM4-8, HadCM3-ICE6GC) are however compatible within error with our ΔNGT_{LGM} of −9.1 ± 0.9 °C (Fig. 6), suggesting that these models may most accurately simulate Western Europe's surface temperatures during the LGM. We speculate that these four models provide the best estimates of future equilibrium warming in this region of the globe. In line with previous conclusions from Zhu et al. (2021), the CESM2-1 model provides an unreasonably large LGM cooling in Eastern Europe (about −20 °C), most likely as a result of a too strong shortwave cloud feedback. As such, the projected future warming in CESM2 (and models with a similarly high equilibrium warming) is likely too large. Direct comparisons between several types of paleoclimate proxies and outcomes of GCM models (as proposed in this study) is a consistent way to evaluate climatic models and their ability to describe past, present, and future climates, including both temperatures and precipitations.

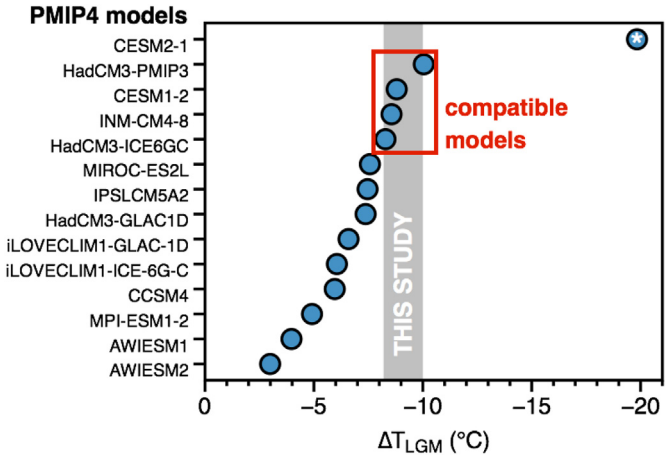

Fig. 6. Comparison of PMIP4 estimates of Eastern France (48°N, 4°E) LGM cooling with our ΔNGT_{LGM} of the Albian aquifer. While most of the PMIP4 models (Kageyama et al. (2021); http://dods.lsce.ipsl.fr/pmip4/db/) predict lower ΔT_{LGM} than observed in the present study, four models (HadCM3-PMIP3, CESM1-2, INM-CM4-8, HadCM3-ICE6GC) appear compatible with our noble gas data. The CESM2-1 model (marked with an asterisk) provides an unreasonably high estimate of LGM cooling in Eastern Europe (−20 °C), consistent with previous findings that this model likely overestimates the amount of equilibrium warming at Earth's surface (Zhu et al. (2021)).

4.5. Quantification of European temperatures during MIS3

In addition to providing important insight into ΔNGT_{LGM}, the noble gas record of the Albian aquifer offers a rare opportunity to constrain European temperatures during MIS3 (between 29 and 42 kyr ago in this dataset). Accurate ^{14}C dating of groundwaters over such timescales is challenging. However, the observation that significant ^{4}He excesses from U—Th decay (computed as the measured ^{4}He concentration minus the equilibrium ^{4}He concentrations obtained from the CE model) are only observed in samples with ^{14}C ages older than 26 kyr ago is an independent, empirical confirmation that these samples are indeed significantly older than Holocene ones (Fig. S4).

During the last glacial period, the North Atlantic region experienced abrupt, north-to-south Dansgaard—Oeschger (DO) climatic oscillations that affected both atmosphere and ocean global circulations (e.g., Andersen et al. (2004)), but whose cause(s) and dynamics remain largely uncertain (e.g., Capron et al. (2021)). These abrupt and potentially globally distributed events have been previously observed during MIS3 in Greenland ice core data (Buizert et al. (2015)), marine sediments from the Atlantic Ocean (e.g., Peterson et al. (2000); Martrat et al. (2007); Deplazes et al. (2013)), and speleothem records (e.g., Wang et al. (2006); Fig. 7). In western continental europe, DO events have been qualitatively recorded in speleothems (Genty et al. (2003)), lake sediments (Thouveny et al. (1994)), and paleosols-loess sequences (Moine et al. (2017)). In principle, we cannot exclude the possibility that some NGTs recorded here during MIS3 (Fig. 3) are also affected, to some extent, by the influence of DO events. This may, at least in part, explain the slight variability of NGTs between ~29 and 42 kyr-old, with for instance the highest NGT (at ~32 kyr ago) corresponding to the # 5.2 DO event recorded in other plaeoclimate archives (Fig. 3). However, high frequency (DO-like) climatic signals are highly unlikely to be preserved in ancient groundwater parcels due to the dispersive and advective nature of mixing during storage at depth. For a typical groundwater dispersivity of 100 m^2/yr and velocity of 1 m/s (Stute and Schlosser (1993)), the e-folding attenuation

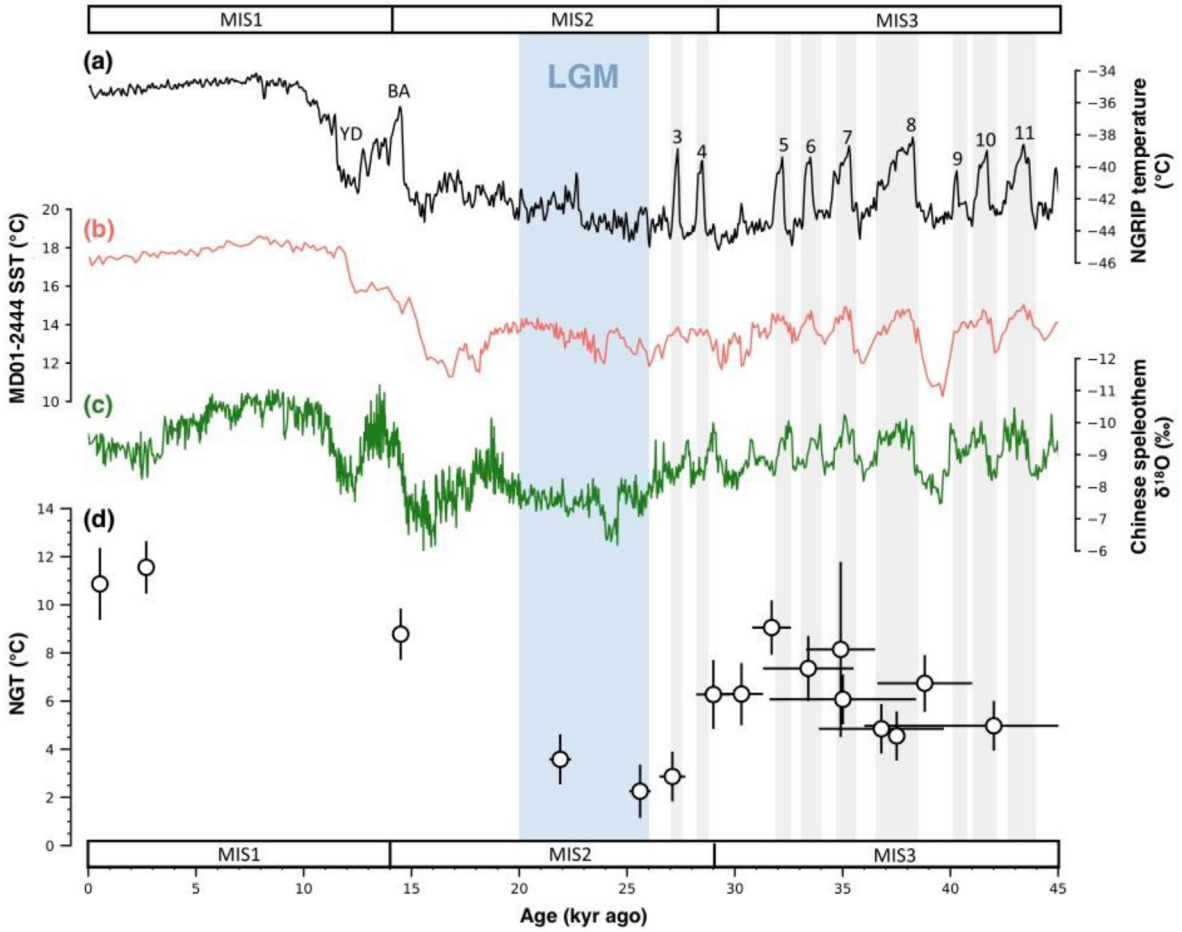

Fig. 7. Comparison of our NGT reconstruction from the Albian aquifer with paleotemperature records of the last ~45 kyr from Greenland ice core, ocean sediments, and speleothem data. (a) Temperature reconstruction from the $\delta^{15}N$ record of the NGRIP Greenland ice core (Kindler et al. (2014), black). **(b)** Sea surface temperature of the iberian margin from the MD01-2444 core (Martrat et al. (2007), red). **(c)** Composite continental $\delta^{18}O$ record from Chinese speleothems (Cheng et al. (2016), green). **(d)** Noble gas paleotemperature (NGT) from the Eastern Paris Basin (white dots, this study). Numbers on the NGRIP Greenland ice core record and vertical gray areas indicate D-O events. Light blue area indicates LGM as defined in this study (26–20 kyr ago). BA: Bølling–Allerød. YD: Younger Dryas.

timescale (i.e., the timescale for a groundwater signal to decrease to 1/e (~1/2.72) of its previous value) of a 1000 yr-long climatic event is for instance ~10 000 years (Fig. S7). After 30 kyr, the magnitude of a DO event-like climatic signal with a period of 1000 yr would therefore be attenuated by a factor >8, implying that the variability potentially induced by the preservation of a DO-like event in groundwater would likely be inferior to the uncetainty on NGT determination (i.e., <1 °C). Here, we compute an error-weighted average of all NGT between 29 and 42 kyr ago of 6.4 ± 0.5 °C, about 4 °C warmer than MIS2. A warmer MIS3 than MIS2 in Eastern Europe may appear inconsistent with the recent proposal that paleo-glacial extents in the North Western French Alps reached their maximum extent during MIS3 rather than during MIS2 (Gribenski et al. (2021)), an observation that may question the respective cooling between MIS3 and MIS2. The good statistical agreement between NGTs reported in this study for MIS3 (Fig. 7) however suggests that the error-weighted average of NGTs between 29 and 42 kyr ago (n = 10, mean = 6.4 ± 0.5 °C) can be used as a quantitative constraint on the extent of cooling during that period of time. Comparing this estimate for the temperature in Eastern France during MIS3 with GCM simulations of MIS3 appears to be another promising avenue to further constrain models of climate evolution since the last glaciation.

5. Conclusion

We have reported a new reconstruction of Eastern France temperature evolution over the last ~40 kyr, using noble gas abundances in the Albian aquifer (Paris Basin) as a quantitative proxy of past temperatures at the time and location of groundwater recharge. This noble gas temperature (NGT) record, independently supported by water stable isotope systematics, depicts a clear glacial-interglacial transition history with mean annual temperatures close to 5 °C during MIS 3, followed by a period of cooling to about 2 °C during the LGM, and then, post glacial warming to Holocene temperatures (~11 °C) between 20 and 10 kyr ago. Altogether, these data indicate an LGM cooling of −9.1 ± 0.9 °C, which supports the notion that continental LGM cooling was more extreme at higher latitudes relative to the tropics (where the ΔT_{LGM} was −5.8 ± 0.6 °C; (Seltzer et al. (2021a)). While our data appear compatible with outputs from the data assimilation of (Tierney et al. (2020)), we find that most climate model simulations of the LGM largely underestimate the extent of glacial cooling in Western Europe during the LGM. Combining our NGT reconstruction with water stable isotopes, we find linear δD/NGT and $\delta^{18}O$/NGT transfer functions of +1.6 ± 0.4‰/°C and +0.18 ± 0.04‰/°C, respectively. Additional inter-proxy and data-model comparisons (using both LGM and MIS3 data as anchor points), as well as new noble gas

records from well-dated archives of variable resolutions, are required to reach a comprehensive assessment of spatial gradients of equilibrium warming across Europe.

Credit author statement

All authors contributed to the manuscript. YR, RP, BM and RK initiated this project and produced the original datasets. DVB, P-HB and AMS processed the data and established the main interpretations. DVB made the tables, figures, and wrote the original draft of the manuscript. All co-authors revised the manuscript and approved its submission.

Declaration of competing interest

The authors declare that they have no known competing financial interests or personal relationships that could have appeared to influence the work reported in this paper.

Data availability

All the data are readily available from the Supplementary Information

Acknowledgements

We thank the two anonymous reviewers for their constructive suggestions that improved the quality of our manuscript. We are greatful to Eawag and ETHZ teams for their effort to operate the noble gas laboratory at ETHZ. Part of this recherche was funded by grant ANR-22-CPJ2-0005-01 to DVB. AS acknowledges funding by NSF grant 2102457. EL acknowledges funding by the French National Research Agency under the “Programme d’Investissements d’Avenir” (ANR-19-MPGA-0001). Funding for open access charge: grant ANR-22-CPJ2-0005-01.

Appendix A. Supplementary data

Supplementary data to this article can be found online at https://doi.org/10.1016/j.quascirev.2023.108123.

References

Aeschbach-Hertig, W., Peeters, F., Beyerle, U., Kipfer, R., 2000. Paleotemperature reconstruction from noble gases in groundwater accounting for equilibration with entrapped air. Nature 405, 1040–1044.
Aeschbach-Hertig, W., Solomon, D.K., 2013. Noble gas thermometry in groundwater hydrology. Adv. Isotope Geochem. 81–122.
Affolter, S., Häuselmann, A., Fleitmann, D., Lawrence Edwards, R., Cheng, H., Leuenberger, M., 2019. Central Europe temperature constrained by speleothem fluid inclusion water isotopes over the past 14,000 years. Sci. Adv. 5.
Andersen, K.K., et al., 2004. High-resolution record of Northern Hemisphere climate extending into the last interglacial period. Nature 431, 147–151.
Andrews, J.N., Lee, D.J., 1979. Inert gases in groundwater from the Bunter Sandstone of England as indicators of age and palaeoclimatic trends. J. Hydrol. 41, 233–252.
Araguás-Araguás, L., Froehlich, K., Rozanski, K., 2000. Deuterium and oxygen-18 isotope composition of precipitation and atmospheric moisture. Hydrol. Process. 14, 1341–1355.
Banerjee, A., Yeung, L.Y., Murray, L.T., Tie, X., Tierney, J.E., Legrande, A.N., 2022. Clumped-isotope constraint on upper-tropospheric cooling during the last glacial maximum. AGU Advances 3, 1–15.
Bartlein, P.J., et al., 2011. Pollen-based continental climate reconstructions at 6 and 21 ka: a global synthesis. Clim. Dynam. 37, 775–802.
Befus, K.M., Jasechko, S., Luijendijk, E., Gleeson, T., Bayani Cardenas, M., 2017. The rapid yet uneven turnover of Earth's groundwater. Geophys. Res. Lett. 44, 5511–5520.
Beyerle, U., Purtschert, R., Aeschbach-Hertig, W., Imboden, D.M., Loosli, H.H., Wieler, R., Kipfer, R., 1998. Climate and groundwater recharge during the last glaciation in an ice- covered region. Science 282, 731–734.
Blard, P.H., Lavé, J., Pik, R., Wagnon, P., Bourlès, D., 2007. Persistence of full glacial conditions in the central Pacific until 15,000 years ago. Nature 449, 591–594.
Blaser, P.C., Kipfer, R., Loosli, H.H., Walraevens, K., Van Camp, M., Aeschbach-Hertig, W., 2010. A 40 ka record of temperature and permafrost conditions in northwestern Europe from noble gases in the Ledo-Paniselian Aquifer (Belgium). J. Quat. Sci. 25, 1038–1044.
Boucher, C., Lan, T., Mabry, J., Bekaert, D.V., Burnard, P.G., Marty, B., 2018. Spatial analysis of the atmospheric helium isotopic composition: geochemical and environmental implications. Geochem. Cosmochim. Acta 237, 120–130.
Buizert, C., et al., 2015. Precise interpolar phasing of abrupt climate change during the last ice age. Nature 520, 661–665.
Byrne, M.P., O'Gorman, P.A., 2018. Trends in continental temperature and humidity directly linked to ocean warming. Proc. Natl. Acad. Sci. U. S. A 115, 4863–4868.
Caillon, N., Severinghaus, J.P., Jouzel, J., Barnola, J.M., Kang, J., Lipenkov, V.Y., 2003. Timing of atmospheric CO2 and antarctic temperature changes across termination III. Science 299, 1728–1731.
Capron, E., et al., 2021. The anatomy of past abrupt warmings recorded in Greenland ice. Nat. Commun. 12, 1–12. Springer US.
Castro, M.C., Jambon, A., De Marsily, G., Schlosser, P., 1998. Noble gases as natural tracers of water circulation in the Paris Basin. 1. Measurements and discussion of their origin and mechanisms of vertical transport in the basin. Water Resour. Res. 34, 2443–2466.
Clark, P.U., Dyke, A.S., Shakun, J.D., Carlson, A.E., Clark, J., Wohlfarth, B., Mitrovica, J.X., Hostetler, S.W., McCabe, A.M., 2009. The last glacial maximum. Science 325, 710–714.
Cleator, S.F., Harrison, S.P., Nichols, N.K., Colin Prentice, I., Roulstone, I., 2020. A new multivariable benchmark for Last Glacial Maximum climate simulations. Clim. Past 16, 699–712.
Coleman, M.L., Shepherd, T.J., Durham, J.J., Rouse, J.E., Moore, G.R., 1982. Reduction of water with zinc for hydrogen isotope analysis. Anal. Chem. 54, 993–995.
Contoux, C., Violette, S., Vivona, R., Goblet, P., Patriarche, D., 2013. How basin model results enable the study of multi-layer aquifer response to pumping: the Paris Basin, France. Hydrogeol. J. 21, 545–557.
Corcho Alvarado, J.A., Leuenberger, M., Kipfer, R., Paces, T., Purtschert, R., 2011. Reconstruction of past climate conditions over central Europe from groundwater data. Quat. Sci. Rev. 30, 3423–3429. Elsevier Ltd.
Craig, H., 1961. Isotopic variations in meteoric waters. Science 133, 1702–1703.
Dansgaard, W., et al., 1993. Evidence for general instability of past climate from a 250-kyr ice-core record. Nature 364, 218–220.
Dansgaard, W., 2012. Stable isotopes in precipitation. Tellus Dyn. Meteorol. Oceanogr. 16, 436.
De Melo Condesso, M.T., Carreira Paquete, P.M.M., Da Silva Marques, M.A., 2001. Evolution of the Aveiro Cretaceous Aquifer (NW Portugal) during the Late Pleistocene and Present Day: Evidence from Chemical and Isotopic Data, vol. 189. Geological Society Special Publication, pp. 139–154.
Deplazes, G., et al., 2013. Links between tropical rainfall and North Atlantic climate during the last glacial period. Nat. Geosci. 6, 213–217. Nature Publishing Group.
Edmunds, W.M., Milne, C.J., 2001. Palaeowaters in Coastal Europe: Evolution of Groundwater since the Late Pleistocene. Geological Society of London.
Ford, H.L., Ravelo, A.C., Polissar, P.J., 2015. Reduced el niño-southern oscillation during the last glacial maximum. Science 347, 255–258.
Froehlich, K., Gibson, J.J., Aggarwal, P.K., 2002. Deuterium Excess in Precipitation and its Climatological Significance. *No. IAEA-CSP–13/*.
Gat, J.R., Gonfiantini, R., 1981. Stable Isotope Hydrology Deuterium and Oxygen-18 in the Water Cycle. International Atomic Energy Agency, Vienna.
Genty, D., Blamart, D., Ouahdi, R., Gilmour, M., Baker, A., Jouzel, J., Van-Exter, S., 2003. Precise dating of Dansgaard – oeschger climate oscillations in western Europe from stalagmite data. Nature 421, 833–837.
Geyh, M.A., 2000. An overview of 14C analysis in the study of groundwater. Radiocarbon 42, 99–114.
Ghadiri, E., Affolter, S., Brennwald, M.S., Fleitmann, D., Häuselmann, A.D., Cheng, H., Maden, C., Leuenberger, M., Kipfer, R., 2020. Estimation of temperature – altitude gradients during the Pleistocene–Holocene transition from Swiss stalagmites. Earth Planet Sci. Lett. 544, 116387. Elsevier B.V.
Ghadiri, E., Vogel, N., Brennwald, M.S., Maden, C., Häuselmann, A.D., Fleitmann, D., Cheng, H., Kipfer, R., 2018. Noble gas based temperature reconstruction on a Swiss stalagmite from the last glacial–interglacial transition and its comparison with other climate records. Earth Planet Sci. Lett. 495, 192–201. Elsevier B.V.
Grant, K.M., et al., 2014. Sea-level variability over five glacial cycles. Nat. Commun. 5. Nature Publishing Group.
Gribenski, N., Valla, P.G., Preusser, F., Roattino, T., Crouzet, C., Buoncristiani, J.F., 2021. Out-of-phase Late Pleistocene glacial maxima in the Western Alps reflect past changes in North Atlantic atmospheric circulation. Geology 49, 1096–1101.
Guiot, J., Pons, A., De Beaulieu, J.L., Reille, M., 1989. A 140,000-year continental climate reconstruction from two European pollen records. Nature 338, 309–313.
Hall, C.M., Castro, M.C., Lohmann, K.C., Ma, L., 2005. Noble gases and stable isotopes in a shallow aquifer in southern Michigan: implications for noble gas paleotemperature reconstructions for cool climates. Geophys. Res. Lett. 32, 1–4.
Heaton, T.H.E., Vogel, J.C., 1981. Excess air" in groundwater. J. Hydrol. 50, 201–216.
Hersbach, H., et al., 2020. The ERA5 global reanalysis. Q. J. R. Meteorol. Soc. 146, 1999–2049.
Ho, S.L., Laepple, T., 2015. Glacial cooling as inferred from marine temperature proxies TEXH86 and UK'37. Earth Planet Sci. Lett. 409, 15–22. Elsevier B.V.
Holland, M.M., Bitz, C.M., 2003. Polar amplification of climate change in coupled models. Clim. Dynam. 21, 221–232.

Hughes, P.D., Gibbard, P.L., 2015. A stratigraphical basis for the last glacial maximum (LGM). Quat. Int. 383, 174–185. Elsevier Ltd.
Ingram, R.G.S., Hiscock, K.M., Dennis, P.F., 2007. Noble gas excess air applied to distinguish groundwater recharge conditions. Environ. Sci. Technol. 41, 1949–1955.
Innocent, C., Millot, R., Kloppmann, W., 2021. A multi-isotope baseline (O, H, C, S, Sr, B, Li, U) to assess leakage processes in the deep aquifers of the Paris basin (France). Appl. Geochem. 131.
James, E.W., Banner, J.L., Hardt, B., 2015. A global model for cave ventilation and seasonal bias in speleothem paleoclimate records. G-cubed 16, 1044–1051.
Jung, M., Aeschbach, W., 2018. A new software tool for the analysis of noble gas data sets from (ground)water. Environ. Model. Software 103, 120–130. Elsevier Ltd.
Kageyama, M., et al., 2021. The PMIP4 Last Glacial Maximum experiments: preliminary results and comparison with the PMIP3 simulations. Clim. Past 17, 1065–1089.
Kipfer, R., Aeschbach-Hertig, W., Peeters, F., Stute, M., 2002. Noble gases in lakes and ground waters. Rev. Mineral. Geochem. 47, 615–700.
Kluge, T., Marx, T., Scholz, D., Niggemann, S., Mangini, A., Aeschbach-Hertig, W., 2008. A new tool for palaeoclimate reconstruction: noble gas temperatures from fluid inclusions in speleothems. Earth Planet Sci. Lett. 269, 408–415.
Klump, S., Cirpka, O.A., Surbeck, H., Kipfer, R., 2008. Experimental and numerical studies on excess-air formation in quasi-saturated porous media. Water Resour. Res. 44, 1–15.
Leng, M.J., Marshall, J.D., 2004. Palaeoclimate interpretation of stable isotope data from lake sediment archives. Quat. Sci. Rev. 23, 811–831.
Loomis, S.E., et al., 2017. The tropical lapse rate steepened during the Last Glacial Maximum. Sci. Adv. 3, 1–8.
Loosli, H.H., et al., 2001. Isotopic methods and their hydrogeochemical context in the investigation of palaeowaters. Geol. Soc. London, Special Pub. 189, 193–212.
Lorius, C., Jouzel, J., Raynaud, D., Hansen, J., Le Treut, H., 1990. The ice-core record: climate sensitivity and future greenhouse warming. Nature 347, 139–145.
Martin, L.C.P., et al., 2020. Antarctic-like temperature variations in the Tropical Andes recorded by glaciers and lakes during the last deglaciation. Quat. Sci. Rev. 247.
Martrat, B., Grimalt, J.O., Shackleton, N.J., De Abreu, L., Hutterli, M.A., Stocker, T.F., 2007. Four climate cycles of recurring deep and surface water destabilizations on the Iberian margin. Science 317, 502–507.
Mazor, E., 1972. Paleotemperatures and other hydrological parameters deduced from noble gases dissolved in groundwaters; Jordan Rift Valley, Israel. Geochem. Cosmochim. Acta 36, 1321–1336.
McManus, J.F., Oppo, D.W., Cullen, J.L., 1999. A 0.5-Million-year record of millennial-scale climate variability in the North Atlantic. Science 283, 971–975.
Millot, R., Petelet-Giraud, E., Guerrot, C., Négrel, P., 2010. Multi-isotopic composition (δ7Li-δ11B-δD-δ18O) of rainwaters in France: origin and spatio-temporal characterization. Appl. Geochem. 25, 1510–1524. Elsevier Ltd.
Moine, O., Antoine, P., Hatté, C., Landais, A., Mathieu, J., Prud, C., 2017. The Impact of Last Glacial Climate Variability in West-European Loess Revealed by Radiocarbon Dating of Fossil Earthworm Granules, pp. 1–6.
Olive, P., 1999. La datation des eaux souterraines à long temps de résidence par le radiocarbone. Mode d'emploi. Hydrogeologie 1, 3–19.
Osman, M.B., Tierney, J.E., Zhu, J., Tardif, R., Hakim, G.J., King, J., Poulsen, C.J., 2021. Globally resolved surface temperatures since the last glacial maximum. Nature 599, 239–244.
Parrenin, F., et al., 2013. Synchronous change of atmospheric CO2 and antarctic temperature during the last deglacial warming. Science 339 (6123), 1060–1063.
Peterson, L.C., Haug, G.H., Hughen, K.A., Ursula, R., 2000. Tropical atlantic during the last glacial rapid changes in the hydrologic cycle of the tropical atlantic during the last glacial. Science 290, 1947–1951.
Petit, J.R., et al., 1999. Climate and atmospheric history of the past 420,000 years from the Vostok ice core, Antarctica the recent completion of drilling at Vostok station in East. Nature 399, 429–436.
Pithan, F., Mauritsen, T., 2014. Arctic amplification dominated by temperature feedbacks in contemporary climate models. Nat. Geosci. 7, 181–184.
Porter, S.C., 2000. Snowline depression in the tropics during the last glaciation. Quat. Sci. Rev. 20, 1067–1091.
Raoult, Y., 1999. La nappe de l'Albien dans le bassin de Paris, de nouvelles idées pour de vieilles eaux. Thèse de doctorat de l'université *Paris VI*, pp. 117–119.
Raoult, Y., Lauverjat, J., Boulegue, J., Olive, P., Bariac, T., 1998. Etude hydrogéologique d'une ligne d'écoulement de l'aquifère de l'Albien dans le bassin de Paris entre Gien-Auxerre et Paris. Bull. Soc. Geol. Fr. 169 (3), 453–457.
Reimer, P.J., et al., 2020. The IntCal20 northern hemisphere radiocarbon age calibration curve (0-55 cal kBP). Radiocarbon 62, 725–757.
Rozanski, K., 1985. Deuterium and oxygen-18 in European groundwaters - links to atmospheric circulation in the past. Chem. Geol. Isot. Geosci. 52, 349–363.
Rozanski, K., Araguās-Araguās, L., Gonfiantini, R., 1992. Relation between long-term trends of oxygen-18 isotope composition of precipitation and climate. Science 258, 981–985.
Seltzer, A.M., Ng, J., Aeschbach, W., Kipfer, R., Kulongoski, J.T., Severinghaus, J.P., Stute, M., 2021a. Widespread six degrees celsius cooling on land during the last glacial maximum. Nature 593, 228–232. Springer US.
Seltzer, A.M., Bekaert, D.V., Barry, P.H., Durkin, K.E., Mace, E.K., Aalseth, C.E., Zappala, J.C., Mueller, P., Jurgens, B., Kulongoski, J.T., 2021b. Groundwater residence time estimates obscured by anthropogenic carbonate. Sci. Adv. 7 (17) eabf3503.
Shakun, J.D., Carlson, A.E., 2010. A global perspective on Last Glacial Maximum to Holocene climate change. Quat. Sci. Rev. 29, 1801–1816.
Shakun, J.D., Clark, P.U., He, F., Marcott, S.A., Mix, A.C., Liu, Z., Otto-Bliesner, B., Schmittner, A., Bard, E., 2012. Global warming preceded by increasing carbon dioxide concentrations during the last deglaciation. Nat. Nat Publish. Group 484, 49–54.
Stadelmaier, K.H., Ludwig, P., Bertran, P., Antoine, P., Shi, X., Lohmann, G., Pinto, J.G., 2021. A new perspective on permafrost boundaries in France during the Last Glacial Maximum. Clim. Past 17, 2559–2576.
Stuecker, M.F., et al., 2018. Polar amplification dominated by local forcing and feedbacks. Nat. Clim. Change 8, 1076–1081. Springer US.
Stute, M., Deak, J., 1989. Environmental isotope study (14C,18O,D,noble gases) on deep groundwater circulation systems in Hungary with reference to paleoclimate. Radiocarbon 31, 902–918.
Stute, M., Forster, M., Frischkorn, H., Serejo, A., Clark, J.F., Schlosser, P., Broecker, W.S., Bonani, G., 1995. Cooling of tropical Brazil (5°C) during the last glacial maximum. Science 269, 379–383.
Stute, M., Schlosser, P., 1993. Principles and Applications of the Iodide Process. Washington DC American Geophysical Union Geophysical Monograph Series, pp. 89–100.
Stute, M., Sonntag, C., 1992. Paleotemperatures derived from noble gases dissolved in groundwater and in relation to soil temperature. Isotopes of noble gases as tracers in environmental studies 111–122.
Sutton, R.T., Dong, B., Gregory, J.M., 2007. Land/sea warming ratio in response to climate change: IPCC AR4 model results and comparison with observations. Geophys. Res. Lett. 34, 2–6.
Thouveny, N., et al., 1994. Climate variations in Europe over the past 140 kyr deduced from rock magnetism. Nature 293, 503–506.
Tierney, J.E., Zhu, J., King, J., Malevich, S.B., Hakim, G.J., Poulsen, C.J., 2020. Glacial cooling and climate sensitivity revisited. Nature 584, 569–573. Springer US.
Tripati, A.K., Sahany, S., Pittman, D., Eagle, R.A., Neelin, J.D., Mitchell, J.L., Beaufort, L., 2014. Modern and glacial tropical snowlines controlled by sea surface temperature and atmospheric mixing. Nat. Geosci. 7, 205–209.
Varsányi, I., Palcsu, L., Kovács, L.Ó., 2011. Groundwater flow system as an archive of palaeotemperature: noble gas, radiocarbon, stable isotope and geochemical study in the Pannonian Basin, Hungary. Appl. Geochem. 26, 91–104.
Višnjević, V., Herman, F., Prasicek, G., 2020. Climatic patterns over the European Alps during the LGM derived from inversion of the paleo-ice extent. Earth Planet Sci. Lett. 538.
Vogel, N., Brennwald, M.S., Fleitmann, D., Wieler, R., Maden, C., Süsli, A., Kipfer, R., 2013. A combined vacuum crushing and sieving (CVCS) system designed to determine noble gas paleotemperatures from stalagmite samples. G-cubed 14, 2432–2444.
Vuillaume, Y., 1971. Application des méthodes isotopiques et hydrochimiques à l'étude de la nappe de l'Albien du bassin de Paris, vol. 71. *Sgn 304 Hyd* 140pp.
Wang, X., Auler, A.S., Edwards, R.L., Cheng, H., Ito, E., Solheid, M., 2006. Interhemispheric anti-phasing of rainfall during the last glacial period. Quat. Sci. Rev. 25, 3391–3403.
Weyhenmeyer, C.E., Burns, S.J., Waber, H.N., Aeschbach-Hertig, W., Kipfer, R., Loosli, H.H., Matter, A., 2000. Cool glacial temperatures and changes in moisture source recorded in Oman groundwaters. Science 287 (5454), 842–845.
York, D., Evensen, N.M., Martınez, M.L., De Basabe Delgado, J., 2004. Unified equations for the slope, intercept, and standard errors of the best straight line. Am. J. Phys. 72, 367–375.
Zhu, J., Otto-Bliesner, B.L., Brady, E.C., Poulsen, C.J., Tierney, J.E., Lofverstrom, M., DiNezio, P., 2021. Assessment of equilibrium climate sensitivity of the community Earth system model version 2 through simulation of the last glacial maximum. Geophys. Res. Lett. 48, 1–10.